

Peripheral tumour targeting using open-source virtual bronchoscopy with electromagnetic tracking: a multi-user pre-clinical study

Herman Alexander Jaeger^{a,b*}, Fabian Trauzettel^{a,b}, Dr. Pietro Nardelli^c, Dr. Federico Daverieux^b, Erlend Fagertun Hofstad^d, Dr. Håkon O. Leira^{e,f}, Dr. Marcus P. Kennedy^g, Dr. Thomas Langø^{d,e}, Dr. Pádraig Cantillon-Murphy^{a,b,h}

^aSchool of Engineering, University College Cork, Cork, Ireland

^bIHU Strasbourg - Institut de Chirurgie Guidée par l'Image, Strasbourg, France

^cApplied Chest Imaging Laboratory, Harvard Medical School, Boston, USA

^dMedical Technology research group, SINTEF AS, Trondheim, Norway

^eSt. Olavs hospital, Trondheim, Norway

^fNorwegian University of Science and Technology, Trondheim, Norway

^gCork University Hospital, Cork, Ireland

^hTyndall National Institute, Dyke Parade, Cork, Ireland

***h.jaeger@umail.ucc.ie**

Peripheral tumour targeting using open-source virtual bronchoscopy with electromagnetic tracking

Objectives. The goal was to demonstrate the utility of open-source tracking and visualisation tools in the targeting of lung cancer.

Materials and Methods. The study demonstrates the first deployment of the Anser electromagnetic (EM) tracking system with the CustusX image-guided interventional research platform to navigate using an endobronchial catheter to injected tumour targets. Live animal investigations validated the deployment and targeting of peripheral tumour models using an innovative tumour marking routine.

Results. Novel tumour model deployment was successfully achieved at all eight target sites across 2 live animal investigations without pneumothorax. Virtual bronchoscopy with tracking successfully guided the tracked catheter to 2-12 mm from the target tumour site. Deployment of a novel marker was achieved at all eight sites providing a reliable measure of targeting accuracy. Targeting accuracy within 10 mm was achieved in 7/8 sites and in all cases, the virtual target distance at marker deployment was within the range subsequently measured with x-ray.

Conclusions. Endobronchial targeting of peripheral airway targets is feasible using existing open-source technology. Notwithstanding the shortcomings of current commercial platforms, technological improvements in EM tracking and registration accuracy fostered by open-source technology may provide the impetus for widespread clinical uptake of electromagnetic navigation in bronchoscopy.

Keywords: lung cancer; tumour; bronchoscopy; electromagnetic navigation, electromagnetic tracking; virtual biopsy; open-source

Introduction

The localisation, targeting and treatment of endobronchial tumours in the outer airways remains one of the most challenging clinical needs in minimally invasive interventions. Despite advances in technological and imaging capabilities, typically less than 30% of primary lung nodules beyond the reach of the non-therapeutic bronchoscope (OD of 3-

5mm) are amenable to diagnosis (1). With the advent of lung cancer screening, small peripheral lung cancers are being detected which often require tissue confirmation prior to surgery (2). Since conventional bronchoscopy alone is not capable of reaching the outer airways due to instrument diameter, hybrid approaches using video bronchoscopy combined with real-time ultrasound (e.g., probe-based radial probe ultrasound [rp-EBUS] delivered through the bronchoscope working channel for peripheral transbronchial imaging, or a bronchoscope with tip-enabled convex probe ultrasound [cp-EBUS], typically for access to the mediastinal lymph nodes) have been developed (3). These approaches may significantly improve local imaging of the nodule but do not consistently improve reach to peripheral targets and do not place the nodule in the context of the pre-operative CT, the usual imaging modality for lung cancer staging.

Electromagnetic tracking for navigated bronchoscopy

Electromagnetic tracking (EMT) has been proposed to provide real-time position and orientation (pose) of the bronchoscope and endobronchial instruments using miniaturised sensors, thereby enabling registration of bronchoscope-deployed instruments to pre-operative CT images (4) or real-time ultrasound (5). EMT has enabled the development of electromagnetic navigation (EMN) (6) as a tool to increase diagnostic yield in outer airway navigation and several commercial platforms exist for both virtual (e.g., Broncus LungPoint) and navigated (e.g., Medtronic superDimension, Veran SPiN Drive) bronchoscopy. While an initial single-centre study on selected patients in an expert setting indicated that EMN could increase clinical yield for endobronchial biopsy in the outer airways by up to 88% when combined with radial EBUS probe (miniature ultrasound probe through the bronchoscope working channel) (7), these initial results were not replicable elsewhere (8–11,4). Currently, manufacturer-sponsored studies are seeking to address replicability in a multi-centre study (12). However, the combination of inconclusive clinical performance and high operating costs means that despite its exciting potential, commercial EMN currently remains limited to select centres. The hypothesis of the present study is that while EMN has the potential to significantly increase clinical yield in peripheral airway nodules, the shortcomings in current technology require innovative approaches to substantially improve clinical usability, flexibility and reduce costs. A second rationale for the study is to test a subjective measurement of EMN accuracy in the *in vivo* setting through the development of novel tumour models and tumour marking protocol which can

successfully replicate the position, material and radiation properties of lung cancer tissue.

Why open-source technology?

Our groups have pursued open-source approaches to both navigated bronchoscopy (13) and electromagnetic tracking (14). Our rationale is that by enabling open-source access to the underlying technology and visualisation tools behind EMN, current technical shortcomings such as low accuracy (i.e., distance to target), high cost and bottlenecks in clinical workflow (e.g., specific CT requirements, time-consuming registration protocols etc.) can be collaboratively tackled. This work represents the first report combining a novel, open-source visualization method for navigated bronchoscopy with open-source electromagnetic tracking of the instrument tip. Pre-clinical validation was achieved by two independent experts (>1000 bronchoscopies performed) in live animals for targeting of multiple targets in the outer airways with a novel tracked catheter deployed through the bronchoscope's working channel. The work also proposes a novel marking protocol using embolization coil deployment, which was used to estimate targeting accuracy in the study, as well as the use of innovative physical tumour models which were targeted in the procedure. Finally, the work highlights the potential for a single procedure "diagnose-and-treat" approach where accurate targeting of suspect peripheral airway nodules may, in the future, enable the immediate deployment of tracked and probe-based endobronchial therapies such as cryotherapy (15), radiofrequency (16,17) or microwave ablation (18).

Materials and methods

This aim of this study was to validate open-source approaches to navigated bronchoscopy with EMN in the pre-clinical setting. A total of four live animal investigations were undertaken, with two preliminary investigations used to identify and address technical shortcomings and define workflow. Two separate investigations, which form the basis of this study, were then undertaken with separate expert users to assess navigational accuracy and technical performance.

Image-guided navigation methods

CustusX (www.custusx.org) is an image-guided diagnostics and therapy research platform dedicated to intraoperative navigation and imaging (13). The platform was

designed as a layered architecture with plugins based on the CTK/OSGi framework, a superbild that manages dependencies and features supporting the image-guided intervention workflow using the ITK and VTK toolkits. Like other open-source medical imaging platforms such as 3D Slicer (19) and MITK (20), CustusX has the flexibility to be utilised in a wide range of clinical settings including neurosurgery, laparoscopic surgery (21), vascular surgery (22) and bronchoscopy (24, 25). An example visualisation palette from the virtual bronchoscopy toolkit is shown in Figure 1.

Electromagnetic tracking for image-guided navigation

Like other open-source platforms, CustusX enables the combination of pre-operative (e.g., MRI or CT) and intra-operative (e.g., ultrasound) imaging modalities using a process called *registration*, which requires the use of either optical or electromagnetic tracking techniques. Registration enables the user to navigate in a virtual environment based on segmented and volume-rendered pre-operative images, which are accurately superimposed with the current tool position and orientation (see yellow arrow in bottom left CustusX view in Figure 1) using real-time tracking information by overlaying with known landmarks (point-based) or volumes (cloud-based). Optical tracking is only effective with line of sight to the navigation target, which has led to the widespread use of OEM electromagnetic tracking platforms such as NDI Aurora for virtual tracking and navigation (25–27). CustusX integrates with electromagnetic tracking platforms like Aurora through the OpenIGTLink protocol (28), an open communications protocol which enables the transmission of status messages, transform and image data between a tracking platform and a computer running CustusX. In this study, a functioning, uni-directional communication link was established between CustusX and the Anser electromagnetic tracking system based on the OpenIGTLink protocol. This enabled real-time visualisation of the catheter tool-tip within the virtual CustusX environment following semi-automatic cloud-registration (29) to pre-operative CT images.

Electromagnetic tracking methods

This study represents the first pre-clinical demonstration of open-source Anser electromagnetic tracking platform (<http://openemt.org>) with virtual image guidance (see Figure 2). Anser is an open hardware EMT platform which uses low-cost acquisition and demodulation techniques and both National Instruments (Austin, Texas) and open-source microcontroller hardware alongside MATLAB support code (Mathworks Corp.,

Natick, Massachusetts). Anser has previously reported pose (position and orientation) accuracy on par with commercial platforms (14). In the present study, the Anser platform was used with a commercial 5 degree-of-freedom (*x-y-z-pitch-yaw*) sensor (part 610099 from Northern Digital Inc., Waterloo, Ontario) with dimensions of 0.5 mm diameter and 8 mm length. It is noted that with appropriate calibration, the platform supports arbitrary electromagnetic sensor coil designs. For this study, two 5 DOF sensors were embedded within a custom-designed steerable catheter, shown in Figure 3, enabling 6 DOF (*x-y-z-pitch-yaw-roll*) pose estimation.

Introduction to in vivo testing procedures

In order to provide a quantitative *in vivo* measure of tracking accuracy, an innovative methodology of tumour targeting was used, as indicated in Figure 4. This is summarised in the following four steps;

- (1) Injection of the tumour model by percutaneous needle injection
- (2) Imaging with CT scan to determine position and volume of each tumour model
- (3) Navigation to each target tumour model using electromagnetic navigation bronchoscopy following registration of the catheter probe within the CustusX virtual environment
- (4) Deployment of a marking coil (embolization coil) at the site of the tumour model, which could be visualised by 3D x-ray. Using the subsequent 3D x-ray, the distance from the tumour model to the marking coil could be accurately measured.

In vivo studies

A female swine (*sus scrofa*, 25-38kg) was used in each investigation, in accordance with national and local ethical approvals (APAFIS #9868-20170511 093041 02 v2, Ministère de l'Enseignement Supérieur de la Recherche et de l'Innovation, 2017). The animal was anaesthetised prior to the procedure (Propofol 4mg/kg and Rocuronium 0.8 mg/kg with 1.15% Isoflurane in an O₂/N₂O mixture) and an 8.5 French cuffed endotracheal tube (Portex Blue Line, Smiths Medical, UK) and catheter mount connector (DAR extendable catheter mount, Covidien) was inserted to facilitate intra-operative ventilation during bronchoscopy. Controlled ventilation was achieved using the Dräger Primus system with blood pressure and heart rate monitoring during the procedure.

Following anaesthesia, a preliminary CT scan was performed (Siemens Somatom Definition AS) with 1 mm slice thickness, 0.7 mm slice overlap with tube parameters of 100 kV and 126 mA. A 240 mm square imaging window was used with 512 x 512 resolution using the ThoraxHR-IR protocol from Siemens. A hard reconstruction filter (B80f) for optimised segmentation performance was employed (30).

Tumour model deployment

The radiopaque tumour model was obtained through a proprietary process (IRCAD France, Strasbourg) based on reported efforts (31) to form a homogenous solution suitable for needle injection. In each case, a total model volume of 1.5 ml was injected at each ‘tumour’ site. In the two pre-clinical animal investigations, four lung sites were targeted in each of the two animals; the caudal (lower) left lobe, the cranial (upper) right lobe, the middle right lobe and the caudal (lower) right lobe. Tumour models were injected to an approximate depth of 2 cm via a double-lumen needle (1.5 mm x 420 mm double lumen tip from Adroit Manufacturing Company, Mumbai, India). This depth is typically favourable to percutaneous CT-guided biopsy in routine clinical practice although we aim to demonstrate the potential utility of bronchoscopic access in this situation. Following injection of the tumour models in each of the two animals, a follow-up CT image was obtained with identical imaging parameters to that of the initial one. This CT confirmed the absence of appreciable pneumothorax in each of the two cases and was also used to characterise each tumour model position and volume. The results are summarised in Table 1 where each tumour model site (x, y) position is measured from the centre of the CT image while z position is measured from the top of the CT topogram. The tumour dimensions ($x \times y \times z$ in mm) upon deployment were measured from the same CT image and these are also included in Table 1. The tumour marker labels *A1- B4* correspond to the eight models placed where the *A* and *B* labels indicate distinct clinical end-users and animals.

Segmentation and registration

The second CT image was also used to perform a segmentation of the lung volume using previously reported methods (23) and the Virtual Bronchoscopy plugin to CustusX. Semi-automatic registration was achieved using the CloudCompare tool (29) and the Bronchoscopy Registration plugin to CustusX following a balanced bronchoscopy airway survey with an EM sensor in the scope channel. A single rigid

registration transformation matrix was calculated during this process. Time domain compensation of the registration to account for errors due to breathing motion was not performed in this study. Following registration, the four injected tumour models were marked with fiducials in CustusX to provide targets for virtual navigation. This facilitated the creation of a virtual pathway from the trachea to the tumour model location in the peripheral airways.

Virtual navigation

The user sequentially navigated to each of the four virtual targets corresponding to the site of the percutaneous tumour model injection. Endobronchial navigation was performed using a novel, 4-tendon catheter (see Figure 3) with two 5-DOF electromagnetic sensors embedded in the catheter tip. The catheter had an outer diameter of 3 mm to fit the 3.2 mm working channel of a standard therapeutic endoscope (Pentax EB-1970TK) while retaining a 1.5 mm working lumen to facilitate instrument and marker delivery to the tumour model site. Once the user had achieved minimal separation from the virtual fiducial marker, as indicated by the tool tip distance indicator in CustusX (see Figure 5), an embolization coil was deployed to mark the target site. In each case, the closest Euclidean distance between the tool tip and the virtual fiducial marker was recorded at the point of marker coil deployment (see Table 1). The marker coil was a 0.035" MR eye embolization coil (Cook Medical, Limerick, Ireland) with a coiled embolus diameter of 2-5 mm and an extended embolus length of 2-4 cm after deployment. Such an approach has previously been proposed as an effective and well-anchored target for airway tumours subject to stereotactic radiation therapy (32). The marker was deployed by means of the working lumen within the tracked catheter shown in Figure 3. Once positioned in the working lumen of the catheter, the marker coil was advanced to the distal tip and deployed from the distal tip using closed endobronchial forceps. Deployment was verified by the inserted length of the forceps.

Measuring targeting accuracy

Targeting accuracy of marker coil deployment was measured using subsequent 3D x-ray (Artis Zeego, Siemens Healthineers, Erlangen, Germany) as indicated in Figure 6. For each marker coil, the closest, furthest and centre-to-centre distance from the tumour model to the centre of the deployed coil was measured using the 3D x-ray image. These

results are included for each tumour model in Table 1. Indicative measurements for tumour model *A3* are shown in Figure 6 where the label *d4* corresponds to the centre-to-centre distance, *d5* is the closest distance and *d6* is the furthest distance between the marker coil and the tumour model. A similar procedure was completed for each of the four tumour models in the two live animal studies. All animals were humanely euthanized by potassium chloride injection under anaesthesia immediately following the procedure.

Results

Tumour model results

Following percutaneous injection of the four tumour models in each of the two reported live studies, no evidence of pneumothorax was seen in the subsequent CT images. This was achieved through careful pre-operative localisation of the optimum deployment area and expert operator deployment. Tumour model position was successful at the four targets. A single tumour model was deployed in each middle left lobe to avoid excessive manipulation in proximity to the animal's heart. The remaining three targets were successfully deployed in the cranial, middle and caudal right lobes in each of the two studies.

The tumour dimensions recorded from subsequent CT and included in Table 1 are representative of the injected volume of 1.5 ml, albeit model *A1* appears larger than expected due to syringe slippage during injection. Major axis lengths for the deployed tumour models ranged from 21.1 mm (labelled *A1*) to 15.5 mm (labelled *A3*). The models are representative of stage IA2-3 lung carcinoma (T1b-cN0M0) non-small cell lung peripheral airway nodules as defined in the TNM classification guidelines (33).

Targeting accuracy results

Post-imaging segmentation and registration of the post-injection CT image with the Anser EMT platform was achieved in each study. As evidenced from the virtual navigation view and subsequent CT images, all eight tumour models deployed in this study lay outside segmented airways. In each case, the user navigated without the assistance of the virtual pathway planner available in the CustusX platform and the tool tip roll-angle orientation was not enabled. Virtual distances from the tool-tip to virtual tumour fiducial between 3.6 mm (label *B4*) and 18.7 mm (label *A3*) were reported in

Table 1. Given the small cohort and user size, any meaningful statistical analysis of results is challenging. However, it is noted that for each user, the closest virtual distance to the tumour fiducial was for targets in the caudal right lobe. The furthest distance to the tumour fiducials occurred in the caudal left (label *B2*) and middle right (label *A3*) lobes where the *A* and *B* labels indicate distinct clinical users. One obvious limitation of the coil-marking procedure employed is that larger embolization coils are more likely to be closer to the tumour target on post-operative images. For this reason, centre-to-centre and furthest distance measures are also included in the results of Table 1.

Following deployment of the marking embolization coils, the resultant closest distance from deployed marker coil to the injected tumour model was found to be between 1.39 mm (model *B4*) and 12.04 mm (model *B2*). Only in one of eight instances (*B2*) did the distance between the tumour model and the deployed marker exceed 10 mm. Furthest distance measurements varied between 14.87 mm (model *B1*) and 30.96 mm (model *A4*), representing the worst case scenarios for targeting accuracy. Although there was weak statistical correlation between the virtual distance to the tumour at marker deployment and the closest distance to the tumour marker from subsequent x-ray images when calculated across all eight tumour models ($r = 0.55$), the shortest virtual distance (model *B4*) corresponded to the minimum closest distance to the tumour model measured by x-ray. Furthermore, in all cases, the virtual distance to the tumour model measured at marker deployment was within the range of the closest and furthest distances to the tumour marker as measured with subsequent x-ray. Notwithstanding the small sample size and limited scope of the current study, this result indicates that the reported position errors of the Anser EMT platform coupled with errors associated with CT registration may be sufficiently small to enable targeting of peripheral nodules, even to targets outside of the segmented airway branches. Current transbronchial needle aspiration (TBNA) techniques will facilitate safe needle access to targets within 10-15mm catheter tip provided the radial displacement lies within the needle curvature. In addition, the capacity to target potential nodules to within 10 mm in seven of eight cases indicates that EMN may play a critical role in decreasing exposure to real-time radiation in patients with lung cancer as well as facilitating rapid image-guided deployment of advanced probe-based endobronchial therapies such as cryotherapy (16), radiofrequency (17,18) or microwave ablation (19) in the near future. While this study targeted tumour models approximately 20mm from the thoracic wall, targeting accuracy will necessarily improve as the diameter of the airway increases closer to the major airway and further

from the percutaneous site (*i.e.*, better segmentation models, easier endobronchial access). Edited video footage of this study is available at <https://youtu.be/5S8pvGGAV8Q>.

It should be noted that in clinical evaluation of EMN, such targeting accuracy is difficult to ascertain because there is no marker placement (except in the case of radiation seeds, and even in these cases, there is no established protocol to estimate the distance from the seed to the tumour target). More typically, studies cite diagnostic yield as a measure of efficacy and this is the approach of recent studies (11,12).

However, this approach conflates technical accuracy of the tracking system with clinical proficiency and biopsy technique. Notwithstanding the expertise of the current clinical investigators, the reported approach may represent significant improvement in the subjective evaluation of targeting accuracy in EMN for navigation to peripheral airway targets because it decouples the system accuracy from clinical proficiency or biopsy technique. We would suggest that our methodology should be tested versus closed source commercial technology to facilitate a true measure of targeting accuracy.

Critical review of the study outcomes

While the study highlights the potential for EMN as a tool for accessing and, potentially, treating peripheral airway tumours, its utility in the absence of real-time radiation for routine clinical practice needs to be further investigated. In this study, CT and x-ray were utilised to provide a ‘gold standard’ of measurement accuracy during endobronchial targeting. Previous clinical studies have conflated targeting accuracy with biopsy technique and clinical proficiency by measuring ‘clinical yield’ and the current method may serve as an important subjective measure of EMN performance prior to clinical evaluation. This study did not seek to identify whether improvements in tracking accuracy and image registration can be rendered small enough in standard clinical practice and this question will need to be investigated as next-generation tracking and navigation tools emerge. The low accuracy, high cost and clinical workflow limitations of current technology make its widespread clinical uptake unlikely. The intention of the authors is to enable next generation technologies, which address these shortcomings, enabling EMN to fulfil its potential in widespread clinical use.

Conclusion

This study represents the first demonstration of Anser EMT system in conjunction with the CustusX intraoperative visualisation platform. This limited pre-clinical study sought to validate the utility of open-source tools in targeting peripheral airway tumour models, indicative of early stage (T1) lung cancer. Utility was quantitatively validated by two independent expert users in separate live animal investigations. Quantitative measures of targeting accuracy indicated that in most cases, endobronchial targeting to within 10 mm was possible. In addition, virtual distance measures to the target site were shown to always lie within the range of subsequently validated distances measured with cone-beam CT. The study, while limited in size and scope, represents a positive indication of the utility of open-source tools in overcoming the current technology roadblocks in EMN of the airways. Furthermore, it points to the potential for electromagnetic tracking to serve as a key enabling technology in deployment of single procedure ‘diagnose and treat’ tools through endobronchial means.

Acknowledgements

The authors would like to acknowledge the help and support of Mr. Mourad Bouhadjar, Mr. Gaël Fouré and the staff at IHU Strasbourg in facilitating pre-clinical investigations as well as Ms. Sophie Pernot and Dr. Bernard Dallemagne who reviewed and prepared the pre-clinical ethical protocols. The authors would like to acknowledge the support of Mr Yohan Mourouveya (Karl Storz GmbH), and that of Mr. Hrishikesh Deo and Ms. Katrin Gerlitz (Pentax Endoscopy) in facilitating access to the equipment used in this study. This work was supported by the Eurostars-Eureka project number 11581, entitled "MARIANA - Image-guided catheter navigation in the outer airways," and by the respective national funding agencies; the Research Council of Norway, the Netherlands Enterprise Agency, and Enterprise Ireland, as well as the IHU Strasbourg feasibility study SCP, Science Foundation Ireland award 15/TIDA/2846, and the Norwegian National Advisory Unit for Ultrasound and Image-Guided Therapy (St. Olavs hospital, NTNU, and SINTEF). The authors would also like to sincerely acknowledge the gracious support of Mr. Jean-Luc Dimarcq, Professor Lee Swanstrom and Professor Jacques Marescaux for hosting this work at IHU Strasbourg.

References

1. Andolfi M, Potenza R, Capozzi R, Liparulo V, Puma F, Yasufuku K. The role of bronchoscopy in the diagnosis of early lung cancer: a review. *J Thorac Dis.* 2016 Nov;8(11):3329–37.

2. Reduced Lung-Cancer Mortality with Low-Dose Computed Tomographic Screening. *N Engl J Med*. 2011 Aug 4;365(5):395–409.
3. Herth F, Becker HD, Manegold C, Drings P. Endobronchial Ultrasound (EBUS) – Assessment of a New Diagnostic Tool in Bronchoscopy for Staging of Lung Cancer. *Oncol Res Treat*. 2001;24(2):151–4.
4. Makris D, Scherpereel A, Leroy S, Bouchindhomme B, Faivre J-B, Remy J, et al. Electromagnetic navigation diagnostic bronchoscopy for small peripheral lung lesions. *Eur Respir J*. 2007 Jun 1;29(6):1187–92.
5. Sorger H, Hofstad EF, Amundsen T, Langø T, Leira HO. A novel platform for electromagnetic navigated ultrasound bronchoscopy (EBUS). *Int J Comput Assist Radiol Surg*. 2016 Aug 1;11(8):1431–43.
6. Eberhardt R, Anantham D, Herth F, Feller-Kopman D, Ernst A. Electromagnetic Navigation Diagnostic Bronchoscopy in Peripheral Lung Lesions. *Chest*. 2007 Jun 1;131(6):1800–5.
7. Eberhardt R, Anantham D, Ernst A, Feller-Kopman D, Herth F. Multimodality Bronchoscopic Diagnosis of Peripheral Lung Lesions. *Am J Respir Crit Care Med*. 2007 Jul 1;176(1):36–41.
8. Ost DE, Ernst A, Lei X, Kovitz KL, Benzaquen S, Diaz-Mendoza J, et al. Diagnostic Yield and Complications of Bronchoscopy for Peripheral Lung Lesions. Results of the AQUIRE Registry. *Am J Respir Crit Care Med*. 2015 Sep 14;193(1):68–77.
9. Reynisson PJ, Leira HO, Hernes TN, Hofstad EF, Scali M, Sorger H, et al. Navigated Bronchoscopy: A Technical Review. *J Bronchol Interv Pulmonol*. 2014 Jul;21(3):242.
10. Mahajan AK, Patel S, Hogarth DK, Wightman R. Electromagnetic Navigational Bronchoscopy: An Effective and Safe Approach to Diagnose Peripheral Lung Lesions Unreachable by Conventional Bronchoscopy in High-Risk Patients. *J Bronchol Interv Pulmonol*. 2011 Apr;18(2):133.
11. Seijo LM, Torres JP de, Lozano MD, Bastarrika G, Alcaide AB, Lacunza MM, et al. Diagnostic Yield of Electromagnetic Navigation Bronchoscopy Is Highly Dependent on the Presence of a Bronchus Sign on CT Imaging: Results From a Prospective Study. *Chest*. 2010 Dec 1;138(6):1316–21.
12. Khandhar SJ, Bowling MR, Flandes J, Gildea TR, Hood KL, Krinsky WS, et al. Electromagnetic navigation bronchoscopy to access lung lesions in 1,000 subjects: first results of the prospective, multicenter NAVIGATE study. *BMC Pulm Med*. 2017 Apr 11;17:59.
13. Askeland C, Solberg OV, Bakeng JBL, Reinertsen I, Tangen GA, Hofstad EF, et al. CustusX: an open-source research platform for image-guided therapy. *Int J Comput Assist Radiol Surg*. 2016 Apr;11(4):505–19.

14. Jaeger HA, Franz AM, O'Donoghue K, Seitel A, Trauzettel F, Maier-Hein L, et al. Anser EMT: the first open-source electromagnetic tracking platform for image-guided interventions. *Int J Comput Assist Radiol Surg.* 2017 Jun;12(6):1059–67.
15. Niu L, Xu K, Mu F. Cryosurgery for Lung Cancer. In: *Modern Cryosurgery for Cancer.* World Scientific; 2011. p. 425–43.
16. Belfiore G, Moggio G, Tedeschi E, Greco M, Cioffi R, Cincotti F, et al. CT-Guided Radiofrequency Ablation: A Potential Complementary Therapy for Patients with Unresectable Primary Lung Cancer—A Preliminary Report of 33 Patients. *Am J Roentgenol.* 2004 Oct 1;183(4):1003–11.
17. Xie F, Zheng X, Xiao B, Han B, Herth FJF, Sun J. Navigation Bronchoscopy-Guided Radiofrequency Ablation for Nonsurgical Peripheral Pulmonary Tumors. *Respiration.* 2017;94(3):293–8.
18. Ridge CA, Solomon SB. IASLC Thoracic Oncology (Second Edition). In: Pass HI, Ball D, Scagliotti GV, editors. *Ablation Options for Localized Nonsmall Cell Lung Cancer.* Philadelphia: Elsevier; 2018. p. 355–362.
19. Pieper S, Lorensen B, Schroeder W, Kikinis R. The NA-MIC Kit: ITK, VTK, pipelines, grids and 3D slicer as an open platform for the medical image computing community. In: *3rd IEEE International Symposium on Biomedical Imaging: Nano to Macro.* 2006. p. 698–701.
20. Wolf I, Vetter M, Wegner I, Böttger T, Nolden M, Schöbinger M, et al. The Medical Imaging Interaction Toolkit. *Med Image Anal.* 2005 Dec 1;9(6):594–604.
21. Langø T, Tangen GA, Mårvik R, Ystgaard B, Yavuz Y, Kaspersen JH, et al. Navigation in laparoscopy--prototype research platform for improved image-guided surgery. *Minim Invasive Ther Allied Technol.* 2008;17(1):17–33.
22. Manstad-Hulaas F, Tangen GA, Gruionu LG, Aadahl P, Hernes TAN. Three-dimensional endovascular navigation with electromagnetic tracking: ex vivo and in vivo accuracy. *J Endovasc Ther Off J Int Soc Endovasc Spec.* 2011 Apr;18(2):230–40.
23. Reynisson PJ, Hofstad EF, Leira HO, Askeland C, Langø T, Sorger H, et al. A new visualization method for navigated bronchoscopy. *Minim Invasive Ther Allied Technol.* 2017 May 30;0(0):1–8.
24. Hofstad EF, Sorger H, Leira HO, Amundsen T, Langø T. Automatic registration of CT images to patient during the initial phase of bronchoscopy: A clinical pilot study. *Med Phys.* 2014 Apr 1;41(4):n/a-n/a.
25. Franz AM, März K, Hummel J, Birkfellner W, Bendl R, Delorme S, et al. Electromagnetic tracking for US-guided interventions: standardized assessment of a new compact field generator. *Int J Comput Assist Radiol Surg.* 2012 Nov 1;7(6):813–8.
26. Condino S, Ferrari V, Freschi C, Alberti A, Berchiolli R, Mosca F, et al. Electromagnetic navigation platform for endovascular surgery: how to develop sensorized catheters and guidewires. *Int J Med Robot.* 2012 Sep 1;8(3):300–10.

27. Nafis C, Jensen V, Beauregard L, Anderson P. Method for estimating dynamic EM tracking accuracy of surgical navigation tools. In: Medical Imaging 2006: Visualization, Image-Guided Procedures, and Display. International Society for Optics and Photonics; 2006. p. 61410K.
28. Tokuda J, Fischer GS, Papademetris X, Yaniv Z, Ibanez L, Cheng P, et al. OpenIGTLink: an open network protocol for image-guided therapy environment. *Int J Med Robot.* 2009 Dec 1;5(4):423–34.
29. Girardeau-Montaut D. CloudCompare - Open Source project [Internet]. CloudCompare 3D point cloud and mesh processing software. [cited 2018 Feb 9]. Available from: <http://www.cloudcompare.org/>
30. Nardelli P, Khan KA, Corvò A, Moore N, Murphy MJ, Twomey M, et al. Optimizing parameters of an open-source airway segmentation algorithm using different CT images. *Biomed Eng OnLine.* 2015 Jun 26;14:62.
31. Blandino A, Macías M, Cantero D. Formation of calcium alginate gel capsules: Influence of sodium alginate and CaCl₂ concentration on gelation kinetics. *J Biosci Bioeng.* 1999 Jan 1;88(6):686–9.
32. Karaman K, Dokdok AM, Karadeniz O, Ceylan C, Engin K. Intravascular Placement of Metallic Coils as Lung Tumor Markers for CyberKnife Stereotactic Radiation Therapy. *Korean J Radiol.* 2015;16(3):626–31.
33. Detterbeck FC, Boffa DJ, Kim AW, Tanoue LT. The Eighth Edition Lung Cancer Stage Classification. *CHEST.* 2017 Jan 1;151(1):193–203.

Table 1. This table indicates the size and location of each of the injected tumour models over the two live animal investigations. In each case the Euclidean distance from the centre of the endobronchial-deployed marker coil to injected tumour model (closest, furthest and centre-centre distance) was measured with reference to the 3D x-ray image, as shown in Figure 6. The virtual distance to the tumour was measured from the virtual imaging platform at the point of marker deployment. This corresponds to the distance between the catheter tool tip (as measured using the Anser EMT system) and the virtual tumour marker placed at the tumour model site within the CustusX environment.

Tumour model label	Lung lobe location	(x, y, z) position [mm]	Tumour size (x x y x z) [mm]	Closest distance to tumour marker [mm]	Centre-centre distance to tumour marker [mm]	Furthest distance to tumour marker [mm]	Virtual distance to tumour at marker deployment [mm]
A1	Cranial right lobe	(-43.5,-5.0,-652)	21.1 x 14.3 x 10.9	2.48	13.13	25.28	9.4
A2	Caudal left lobe	(64.5,-7.5,-694.1)	18 x 11.8 x 12.1	6.95	16.23	23.55	12.8
A3	Middle right lobe	(-42.9,-10.8,-682.2)	15.5 x 16.5 x 19.3	3.79	16.88	28.23	18.7
A4	Caudal right lobe	(-49.2,-17.6,-706)	16.2 x 12.7 x 15.9	8.07	18.98	30.96	8.3
B1	Cranial right lobe	(-68.8, -10.0, -583.5)	16.7 x 10.7 x 12.3	1.97	7.19	14.87	9.0
B2	Caudal left lobe	(49.5,-3.0, -578.6)	18.3 x 10.1 x 0.98	12.04	19.76	28.51	18.4
B3	Middle right lobe	(-53.2,-23.1, -533.8)	16.7 x 15.8 x 13.7	5.54	17.1	29.12	8.7
B4	Caudal right lobe	(-72.1, -27.9, -594.7)	15.6 x 9.6 x 15.3	1.39	11.15	22.88	3.6

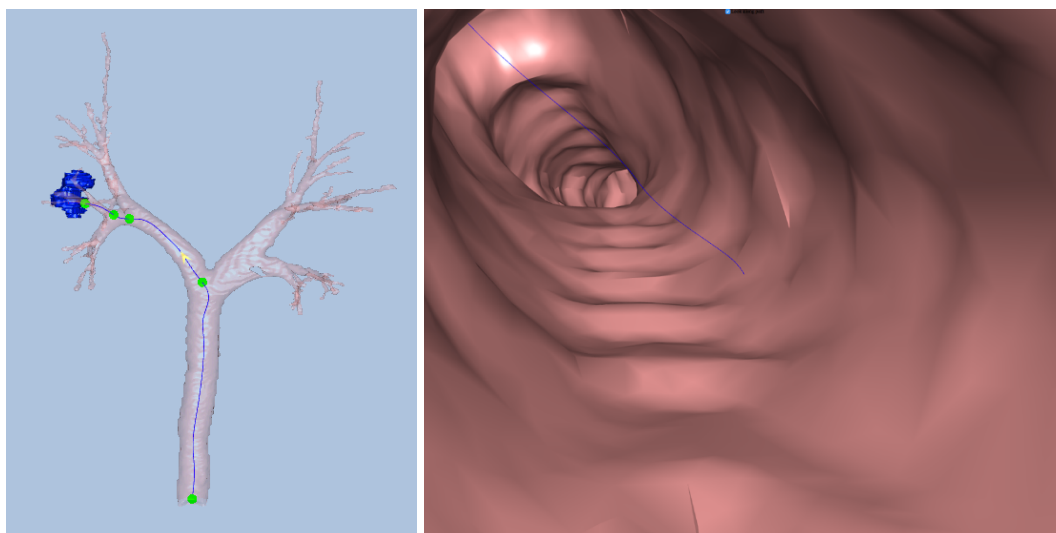
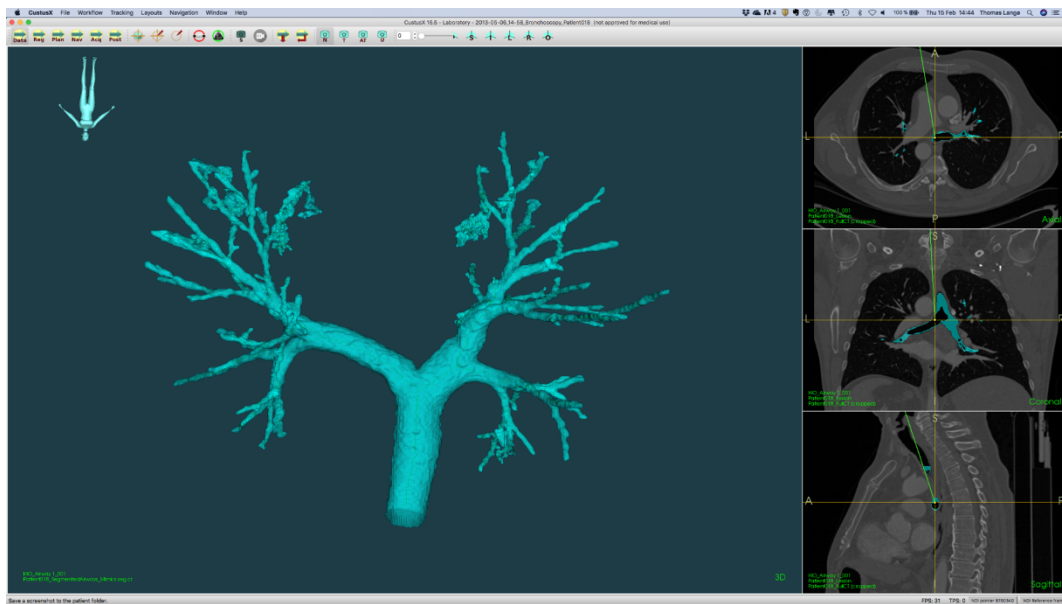


Figure 1. Navigation platform/system monitors display examples from the CustusX navigated bronchoscopy environment using a segmented 3D airway model (top left and bottom left) processed from preoperative patient CT (www.custusx.org) (13). Virtual bronchoscopy (bottom right) and axial, sagittal and coronal displays (top right) are available. Segmented models from the CT can be overlaid the orthogonal CT planes as shown and the centerline is extracted automatically with the airway lumen. Path to target is calculated automatically after defining the target manually (example: blue tumour in bottom left image).

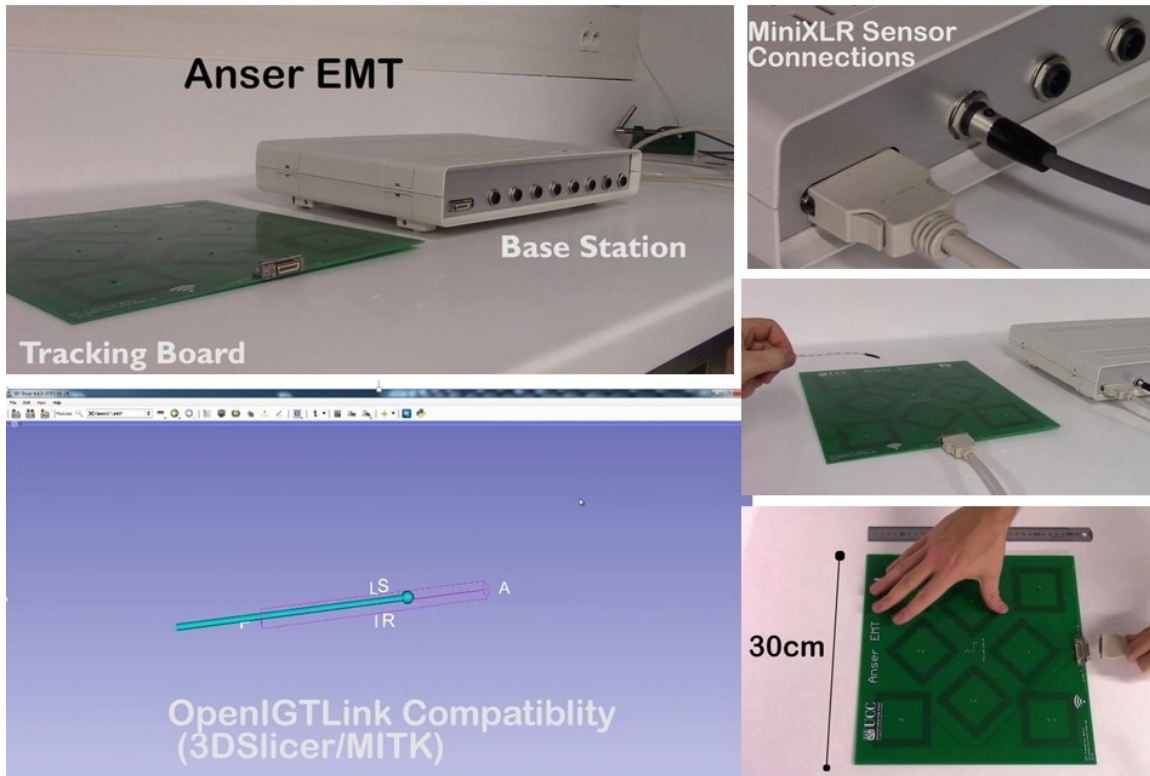


Figure 2. The Anser EMT (www.openemt.org) platform comprises a base station, a 30 cm² tracking board and up to 15 5-DOF (or 8 6-DOF) sensors which are connected via miniXLR adapters to the base station. The system is fully compatible with OpenIGTLink using supporting Matlab software and estimated system latency in this mode is less than 35ms.

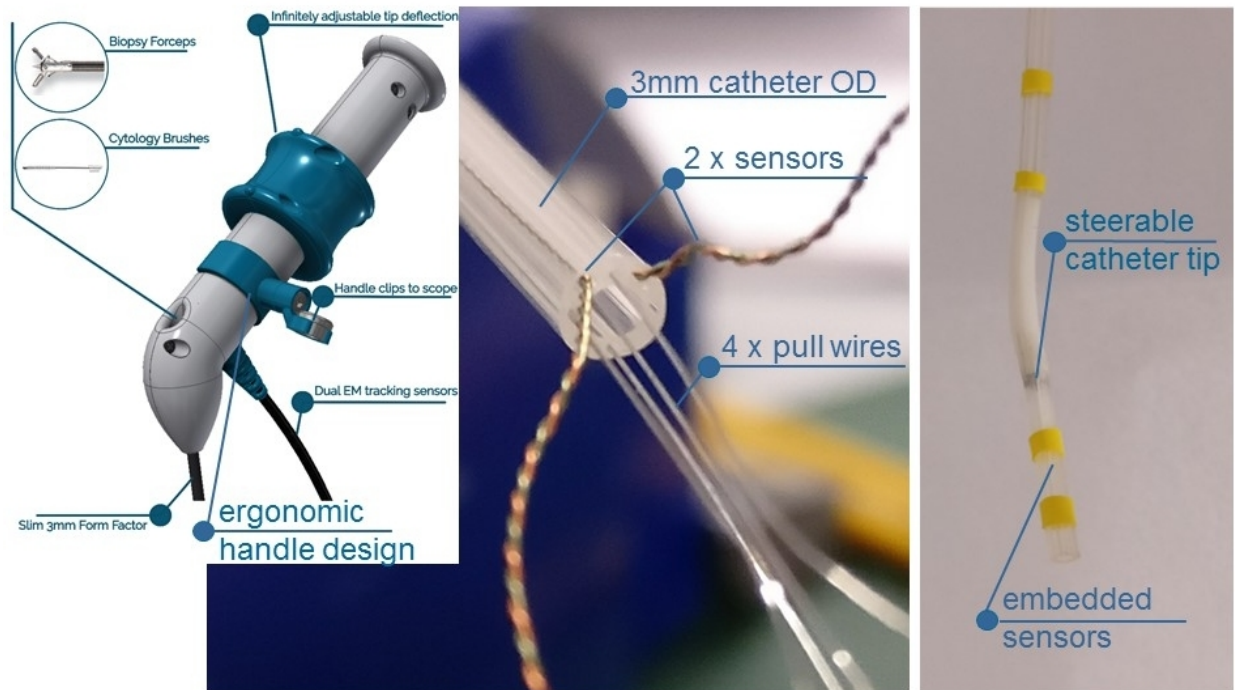


Figure 3. A custom-design electromagnetically tracked catheter with steering capabilities was used in this study. Two 5 DOF electromagnetic sensors were embedded in the catheter wall to enable real-time tracking, while 4 pull-wire tendons enabled steering with a mechanical handle. The catheter measured 3mm outer diameter with a 1.5mm working lumen for deployment of biopsy forceps, cytology brushes or other tools such as the marking coils used in this study. Note that the yellow bands shown on the catheter tip were added for visualisation and characterisation purposes only.

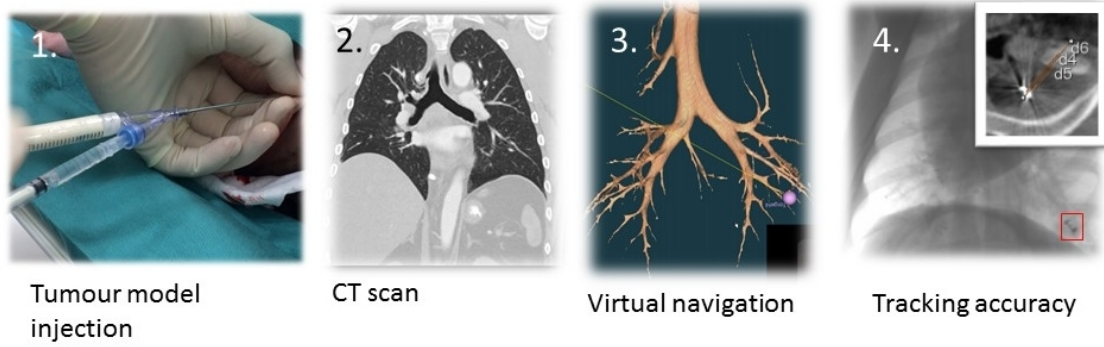


Figure 4. Tracking accuracy was measured by endobronchial placement of a marking coil at each tumour model site. The distance between the deployed marking coil and the injected tumour model provided a quantitative and objective measure of targeting accuracy in the study.

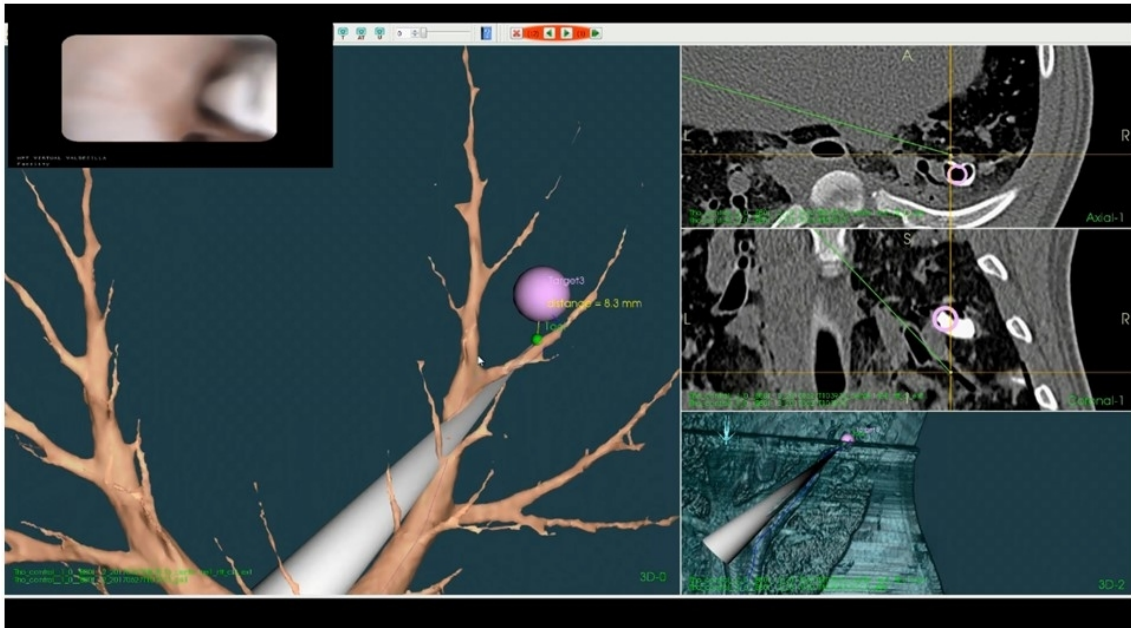


Figure 5. Virtual navigation of the tracked catheter is shown to tumour model *A4* located in the caudal (lower) right lobe. Virtual navigation was achieved to within 8.3 mm of the virtual fiducial in this case. CT image palettes on the right of the screen clearly indicate the injected tumour model which coincides with the position of the virtual fiducial marker. The marking coil is deployed through the working lumen of the tracked catheter. It should be evident that the endoscopic video view (top right inset) is not useful in navigating to such peripheral and transbronchial targets as the bronchoscope diameter (6.3 mm) is too large to pass to the outer airways (2-4 mm).

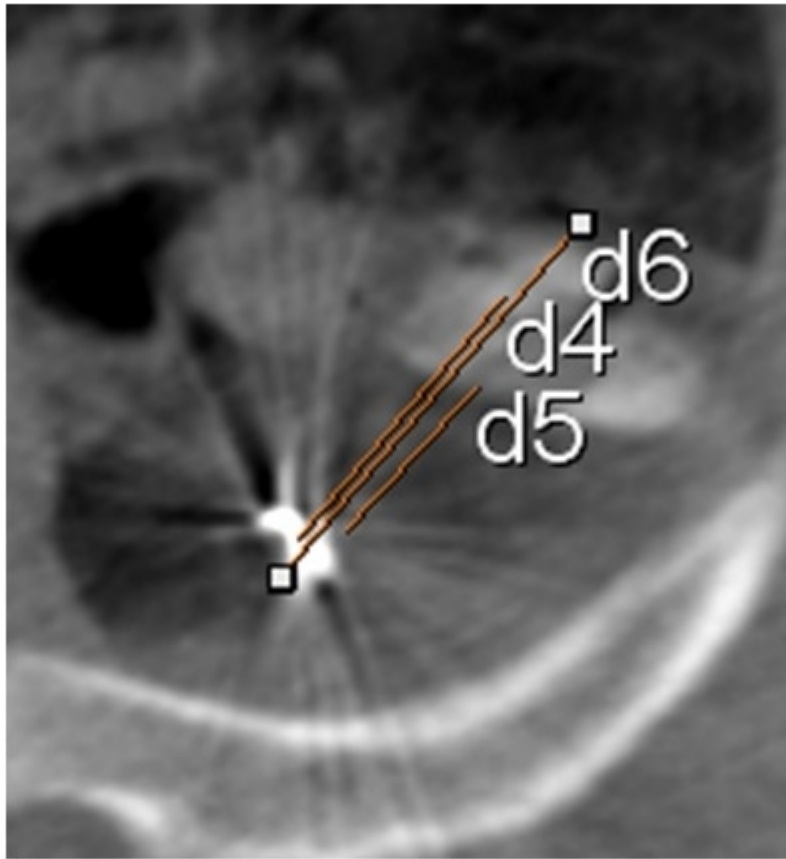


Figure 6. The Euclidean distance between the marking coil and the deployed tumour model was manually measured using the PACS ruler tool from 3D x-ray. The resultant images facilitated the measurement of centre-to-centre (labelled $d4$ in this image), closest (labelled $d5$) and further ($d6$) distances between the deployed marker coil and the tumour model. This procedure was repeated for each of the eight tumour models described in Table 1.